SPECIAL PROJECT FINAL REPORT

All the following mandatory information needs to be provided.

Project Title: **Atmospheric Boundary Layer processes in Complex Terrain**

Computer Project Account: SPESTURB

Principal Investigator(s):   JOAN CUXART RODAMILANS

Affiliation: UNIVERSITAT DE LES ILLES BALEARS (UIB)

Other researchers: MARIA A. JIMÉNEZ
IMEDEA (UIB-CSIC)

Start date of the project: 1st January 2012

Expected end date: 31st December 2014

Summary of project objectives

(10 lines max)

The main aims of this project are to understand and characterize the circulations within the Atmospheric Boundary Layer in complex terrain through the combined use of experimental data and high-resolution numerical simulations. The main topographical features of a region are a key to determine the local circulations, and their effects are predominant under weak general pressure gradients. We have chosen areas in Western Europe with well-defined orographic forcings, such as the northern side of the Pyrenees, the Reuss valley in Switzerland or the Mallorca Island. These locations have experimental data of good quality, allowing us to study the effects of terrain heterogeneity in a 24-hour cycle, with a special focus on the nocturnal part and the evening and morning transitions. Simulations at very high vertical resolution and with nested domains with horizontal resolutions from the kilometric to the decametric scales are performed on the ECMWF computing system.

Summary of problems encountered (if any)

(20 lines max)

Experience with the Special Project framework

(Please let us know about your experience with administrative aspects like the application procedure, progress reporting etc.)

The procedures to apply a special project are clearly stated on the ECMWF web page, as well as the deadlines and forms for the progressing/final reports. Therefore, we think that there is no confusion about these procedures.

Summary of results

(This section should comprise up to 10 pages and can be replaced by a short summary plus an existing scientific report on the project.)

This project is the continuation of a former one devoted to the study of the stably stratified boundary layer (SPESTURB, 2002-2011) which gradually evolved into the study of the Atmospheric Boundary Layer (ABL) over complex terrain in weak general pressure gradients, allowing us to inspect the effect of the terrain-induced flows over the ABL characteristics.

That project had a first part, when Large-Eddy Simulations of the idealized Stably stratified ABL were performed with the Meso-NH model (Lafore et al., 1998), first analysing some characteristics of the modelled regime, such as anisotropy and intermittency (Jiménez and Cuxart, 2005), and then forcing the regime with a Low-Level Jet (LLJ) such as the one observed in the Duero valley (Cuxart and Jiménez, 2007), which proved that the presence of a LLJ changes completely the behaviour of the nocturnal ABL, leading to weaker stratification. Some of these findings were shared in the frame of the GABLS community (Beare et al., 2006).

The second part of the project was mostly devoted to understand the formation and evolution of the LLJs in complex terrain, choosing areas with good data and relatively simple geometry. Analysis of the mesoscale flow organization and cold pool formation was made for the Duero basin in winter, where the CIBA experimental site is located (Bravo et al., 2008; Martínez et al., 2010). In Mallorca, the interaction of sea and land breezes and topography is very important and the time-space evolution of the nocturnal flows was inspected (Cuxart et al., 2007; Martínez and Cuxart, 2007; Cuxart, 2008; Martínez and Cuxart, 2009), also with the development of verification tools based on satellite images (Jiménez et al., 2008).

More recently, in the Ebro basin, we analysed the role of narrow valleys and extensive mountain walls in the generation of within-basin circulations, with special attention to the evolution of basin-wide radiation fog and the role of large irrigated areas (Cuxart and Jiménez, 2012), also with the extensive use of satellite imagery and instrumental data (Martínez et al, 2008; Cuxart et al., 2012). Since 2011 we have devoted our efforts in the understanding of the interaction of the Pyrenees and the Garonne basin in the frame of the BLLAST cooperative effort (Jimenez and Cuxart, 2014; Lothon et al., 2014). In all of these cases, the presence of a LLJ enhances turbulent mixing and limits (in the model) the formation of a very strong nocturnal inversion.

From the beginning of this new project, in 2012, we are concentrating our efforts in four main lines: i) interaction mountain range and plain in the Pyrenees; ii) sea and land breezes in Mallorca; iii) strong cooling inversion in Mallorca and Lleida; iv) 24-h cycle in the Swiss Reuss valley and v) surface energy budget studies.

1) Topographically generated winds in the northern central Pyrenees

In this area we want to explore the 24-h cycle of mountain and valley winds adjacent to a large plain, taking advantage of an important experimental campaign in June and July 2011. The Boundary Layer Late Afternoon and Sunset Transition (BLLAST) project organized an experimental field campaign in Lannemezan (over a plateau to the north of the central Pyrenees). A large number of scientific teams gathered experimental data that can now be used to check the goodness of our methodology already tried in 2011. The description of this campaign is found in Lothon et al. (2014).

In order to prepare the experimental field campaign, a numerical study of the downslope winds in the central Pyrenees was performed (Jiménez and Cuxart, 2014) to identify the spatial and temporal scales of the downslope and down-valley winds present in the Lannemezan area (Fig. 1.1).
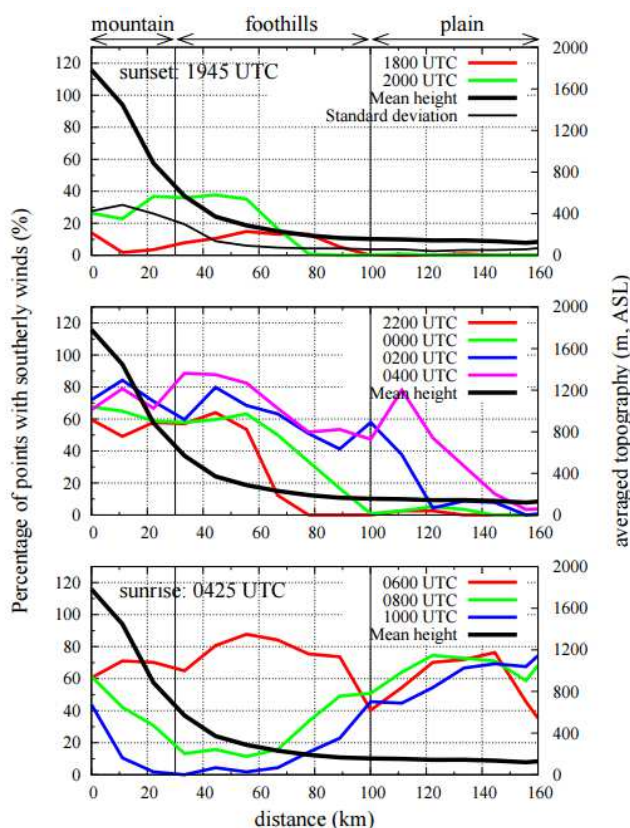

Figure 1.1. Percentage of the grid points with southerly wind (wind direction below 200m AGL ranging between 120º - 240º) along a line perpendicular to the Pyrenees. This percentage is plotted every 2 hours from 30 June 2010 at 1800 UTC to 1000 UTC of the next day. The averaged topography of the whole line (in m, ASL) for each distance from the Pyrenees is shown with a black thick line and the standard deviation with a thinner black line (see right-hand side scale). The vertical lines indicate the three regions: mountain, foothills and plain.

For an IOP event during the BLLAST campaign that lasted four days (from 29th June 2011 at 0000 UTC to 2nd July 2011 at 0000 UTC) a mesoscale simulation with 3 nested domains (at horizontal resolutions of 2km, 400m and 80m, centered in Lannemezan, see Fig. 1.2) has been made. It rained during the first 2 days and clear skies and weak pressure gradient conditions were observed during the last two days. The 1st July 2011 is taken to analyse the topographically generated winds (upslope during the day and downslope during night) in the area of Lannemezan.

(a) Domain 1
(2km x 2km resolution)

(b) Domain 2
(400m x 400m resolution)

(c) Domain 3
(80m x 80m resolution)
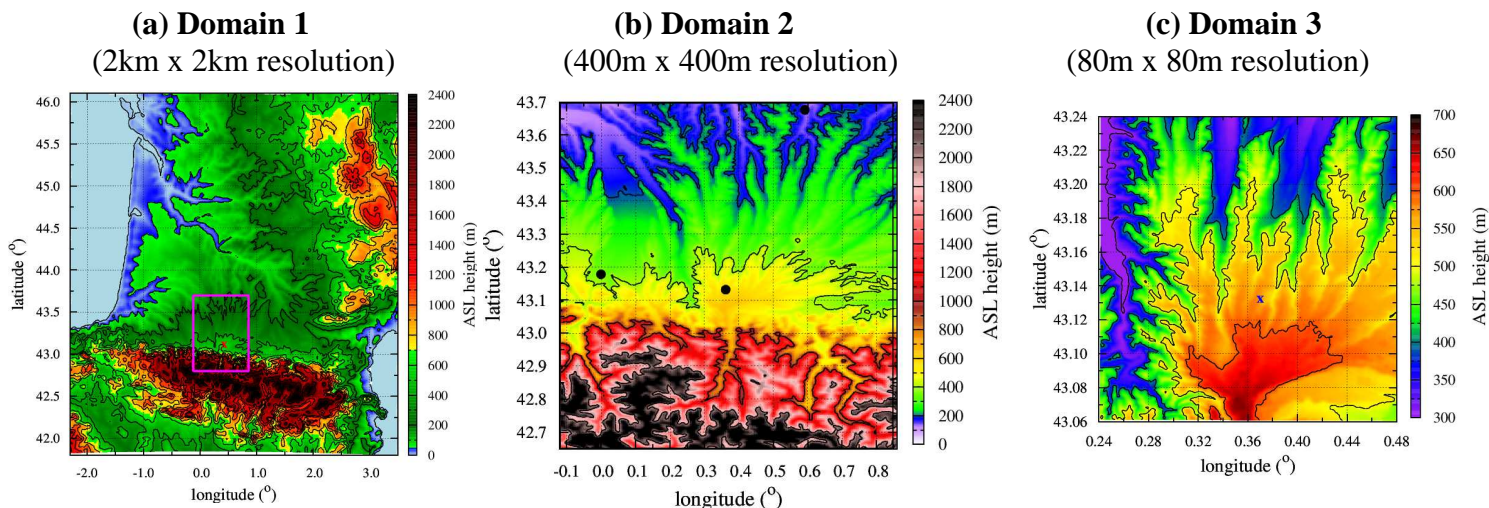
Figure 1.2. Topography of the 3 nested domains of the simulation of an IOP during the BLLAST field campaign: In (b) the location of Lannemezan is indicated with a dot and in (c) with a blue cross.

With the data from the 2011 experimental field campaign it is possible to check how realistic the model results are. It is found that downslope and down-valley winds are generated during the night for any model resolution, although there are differences in the wind direction at lower levels (for instance at 50m a.g.l., as it is seen in Fig. 1.3), being the 400m resolution run closer to the observations. When the model outputs at 400m and 80m resolutions (not shown) are compared, it is found that there are not substantial differences between them although the surface temperature field is more heterogeneous at 80m resolution (Fig. 1.4). An analysis of the temperature heterogeneities at different spatial scales over Lannemezan using model outputs (3 nested domains) and observations (UAV, satellite and thermal cameras) is under progress and the manuscript will be submitted to ACP by the end of this year (Cuxart et al. 2015).
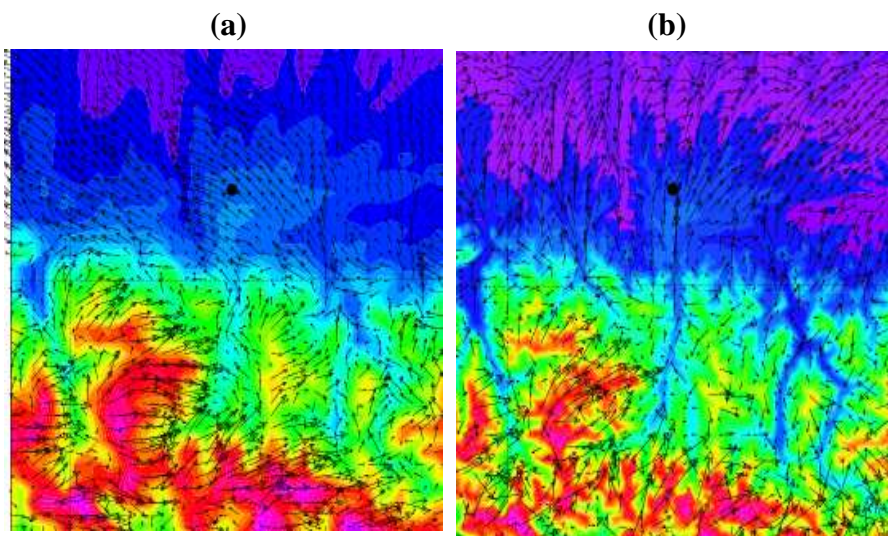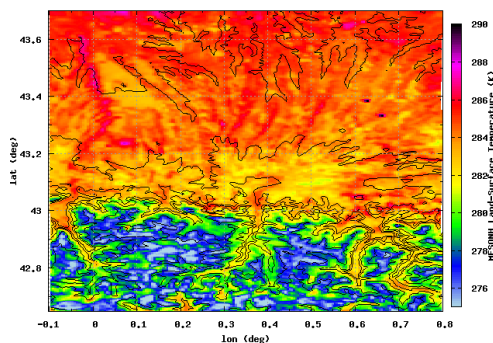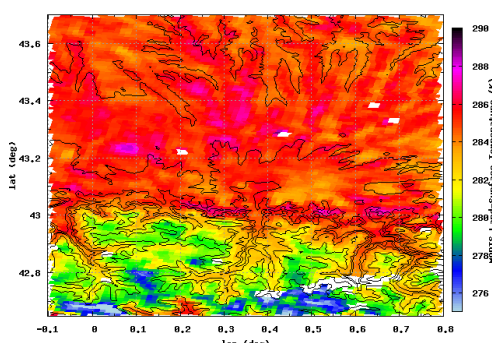
(a)　　　　　　**(b)**

Figure 1.3. Wind vectors at 50 m (a.g.l.) at 2330 UTC on July 1st, 2011 for (a) domain **1** with a zoom over the domain **2** area and (b) for domain **2**.
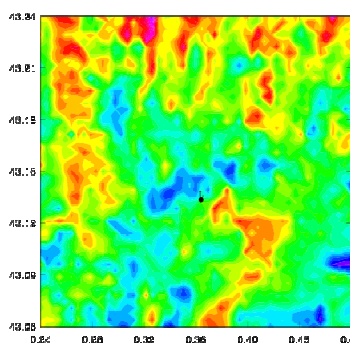
(a) Domain 2 (MesoNH)

b) Domain 2 (MODIS)

(c) Domain 2
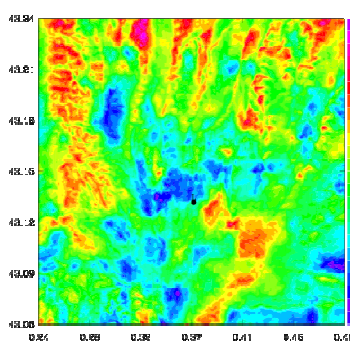**(zoom over Lannemezan plateau)**

(d) Domain 3

Figure 1.4. LST at 0200 UTC on July 2nd, 2011 for (a) domain 2 (MesoNH) and (b) derived from the MODIS satellite. The same as (a) in (c) but for a zoom covering Domain 3 in order to compare to (d) the temperature field obtained in Domain 3.

The verification of the model outputs is made through the use of satellite images and data from the BLLAST experiment. Fig. 1.4 shows that the model is able to reproduce the satellite-derived surface temperature patterns although it is about 2 K warmer at night. However, the temperature difference between mountain-plain is nearly the same (6-7 K).

The time series of the vertical profiles for the wind speed and the temperature (Fig. 1.5) show a maximum of wind speed at lower levels (around 30 m, a.g.l. at 2300-0000 UTC and around 100 m a.g.l. at 0300-0500 UTC). The earliest one has southern direction (down-valley winds generated in the Aure valley) is stronger for the 400 m resolution domain in agreement to observations. Thus, there is more shear and the mixing makes that the cooling of the surface layer is reduced, although this cooling is more concentrated at lower levels in the 400m/80m runs than for the coarser resolution. As a result, the simulation at 400m resolution is properly capturing the downslope and down-valley winds that reach Lannemezan (compromise between computational resources and results closer to the observations). At lower levels (Fig. 1.6) the temporal evolution of the observed temperature and wind from the 60m tower is well captured by the model.

It is important to mention that the inner domain at 80m is computationally very expensive. We only run it for short periods that are close to stationarity. With the support of the computing units from AEMET the simulation with the 3 domains is run from 2300 UTC to 1000 UTC of the next day, when the turning from downslope to upslope winds is completed. To have a good representation of the surface characteristics at high resolution, we have built higher resolution topography from the *srtm* database at 90m (http://srtm.csi.cgiar.org). However, other terrain characteristics are not available at a resolution higher than 1 km and we are currently inspecting the impact of these surface features (see section 5).

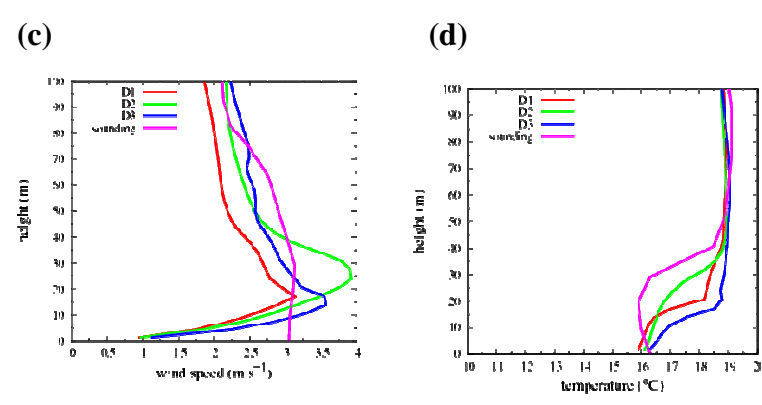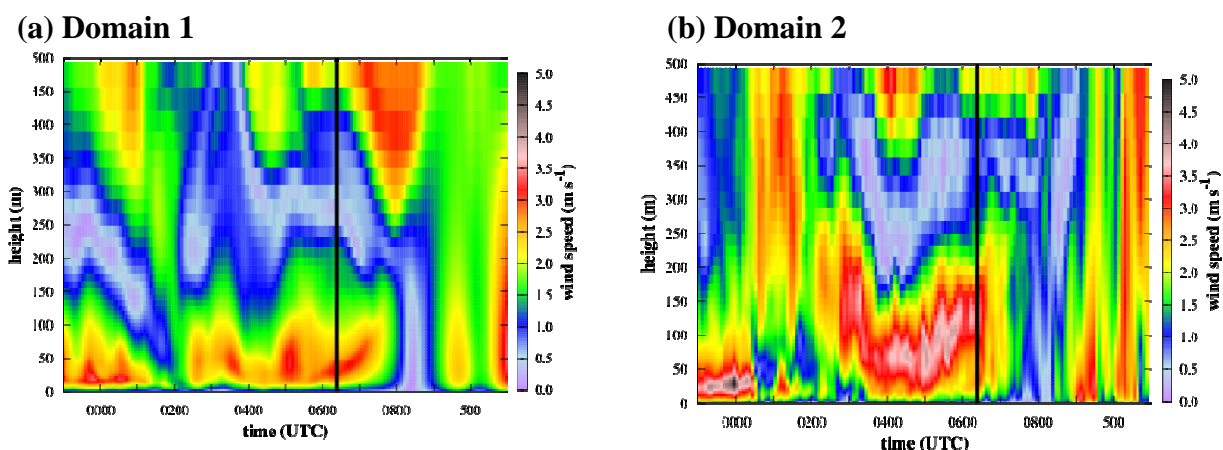**(a) Domain 1**

(b) Domain 2

(c)

(d)

Figure 1.5. Time series of the vertical profiles of the wind speed obtained from domains (a) 1 and (b) 2 in Lannemezan. In (c) and (d) the modelled and observed vertical profiles at 2330 UTC.

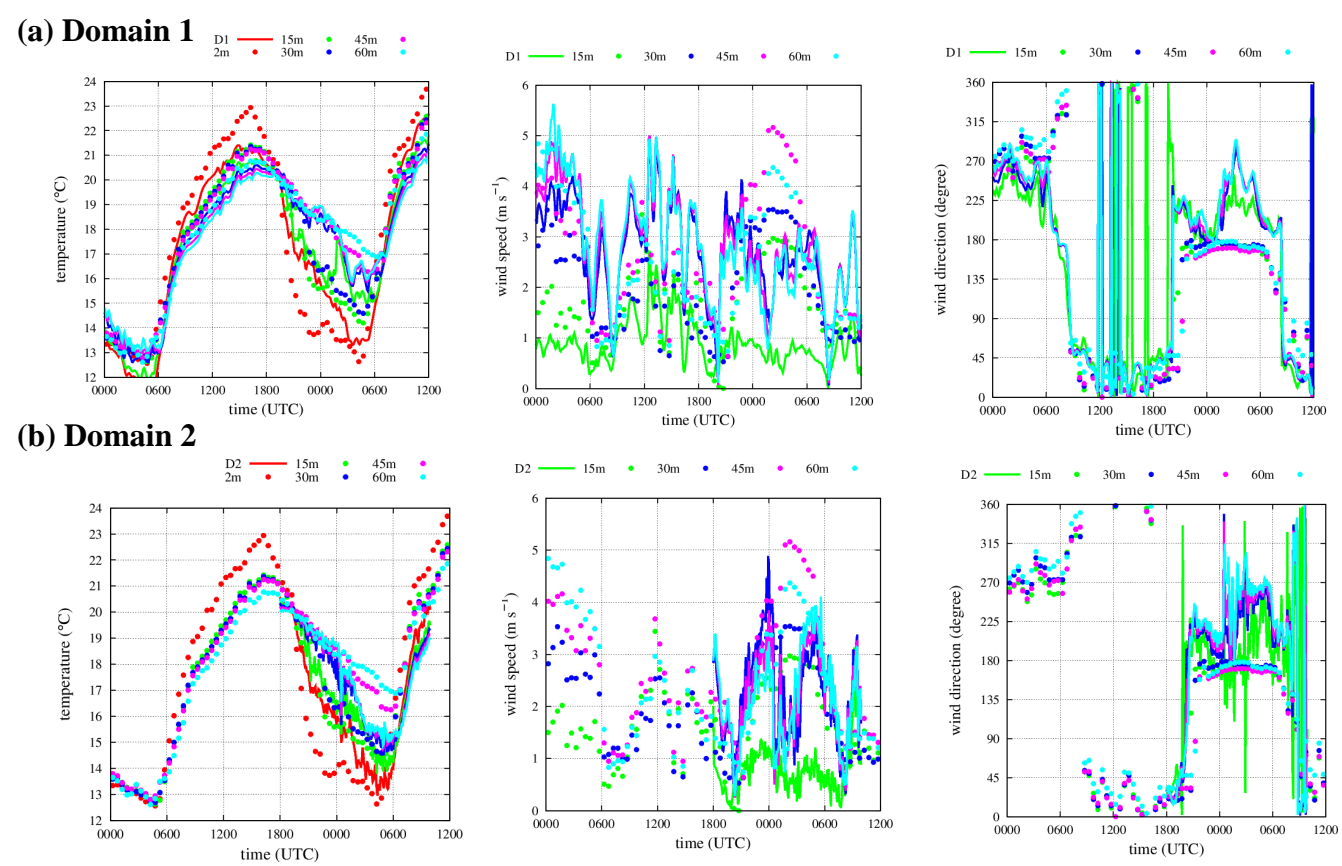**(a) Domain 1**

(b) Domain 2

Figure 1.6. Comparison of the model results (domains 1 and 2) with the 60m tower data.

Another IOP from the BLLAST experimental field campaign has been considered to evaluate the performance of different models (Arome, Arpege, WRF and MesoNH). We have participated with the MesoNH model. The setup is similar to the previous simulations described for this area. The horizontal resolution is 3 km x 3 km and the vertical 10 m close to the surface and stretched above. Different initial and boundary conditions are evaluated as well as different parameterizations. The preliminary results are shown in Figure 1.7. Although there is a large spread in the modelled latent and sensible heat fluxes the observations have a similar pattern. The MesoNH model is able to reproduce the boundary layer height and the temperature profile observed from the sounding. This work is still in progress and results will be submitted to the ACP special issue (Pino et al., 2015).
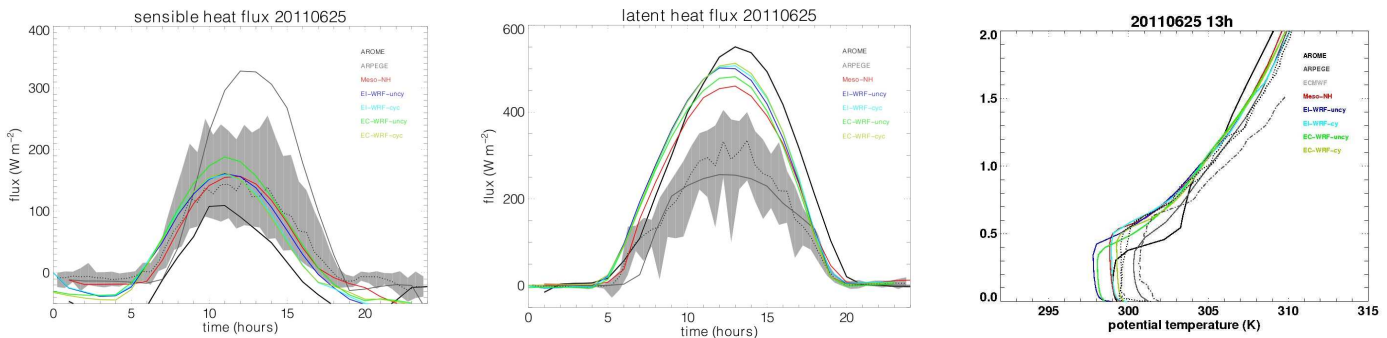

Figure 1.7. Time series for (a) H and (b) LE observed (mean value and standard deviation in grey) and obtained from the different models that participate in the intercomparison. (c) Vertical profiles of the potential temperature at 1300 UTC. The observed soundings are also included (dashed lines).

2) Characterization of the land- and sea-breezes in Mallorca.

Mallorca is where we study the time-space evolution of the land- and sea-breezes in a basin. The Campos basin is taken (see Fig. 2.1) where it is planned a series of experimental field campaigns (field site indicated with a red dot in Fig. 2.1). The first one was in September 2013 (Mallorca Sea Breeze, MSB13, Jiménez et al., 2015), the second in June 2014 (MSB14) and a third one during summer 2015. Climatologically, the sea-breeze is observed by the surface stations of AEMET about 50% of the days of the year. Between April and October, if the temperature difference between sea and land is strong enough, and under weak pressure-gradient conditions, the sea-breeze is formed. The duration and intensity of the sea-breeze will depend on the temperature difference between land and sea, among other factors.

In order to start characterizing the sea-breeze, a mesoscale simulation has been performed over the island of Mallorca, with a setup similar to the one described in Cuxart et al., (2007). Two nested domains are taken. The outer one covers the Balearic Islands at 5km resolution and the inner one is centered in Mallorca (see Fig. 2.1a). Clear-skies and weak synoptic pressure gradient conditions are taken (simulated period from 4th June 2010 at 1200 UTC to 6th June 2010 at 0000 UTC).
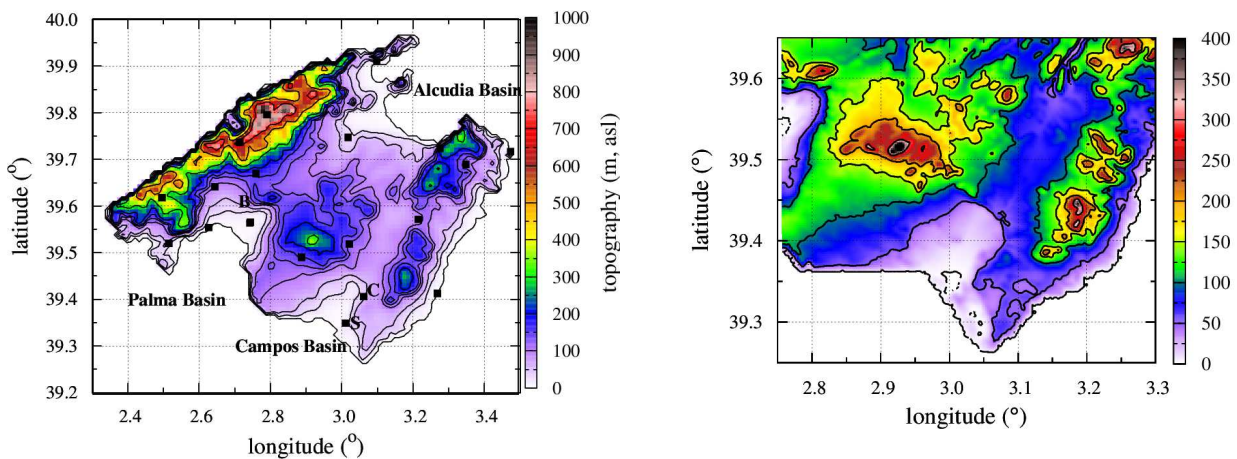

Figure 2.1. Topography of (a) the inner domain (at 1km resolution) of the run and (b) the 3rd nested domain and 250m resolution (only for MSB14 runs).

Fig. 2.2 shows that during the night downslope winds are generated in the three main basins and the wind flows out from the mountains to the sea, following the terrain. During the day, the wind has an opposite direction and it flows from the sea to the land, through the three main basins. The complete analysis of the sea-breeze in Campos is found in Cuxart et al. (2014). From the model outputs it is seen that the sea breeze has 5 phases, indicated in table 2.1.

Phase	Interval (UTC)	Patterns	Budgets and processes in surface layer over land		
			T	TKE	V
Previous	0430–0730	Cold offshore wind; initial warming of land; LST < SST	Warming over land uncompensated	Thermal production	Negative pressure gradient (toward sea)
Preparatory	0730–0900	Offshore wind stops; LST > SST; CBL building over land; wind inland just over the coastline	Initial inland cooling close to the coast	Thermal production	Pressure gradient changes sign
Development	0900–1200	Wind inland; front speed ≈ 3 m s⁻¹; max turbulence; LST ≫ SST	Cooling by marine advection equilibrates radiation/turbulence warming	Shear production starts and becomes larger than thermal production at the end	Acceleration inland; main terms: pressure and turbulence
Mature	1200–1500	Wind, TKE, and LST–SST constant; T slowly decreasing	Marine advection compensates turbulence/radiation	Shear production larger than thermal production	All terms decrease with time
Decay	1500–1900	Wind decreases, turning near the coast; T and TKE decrease; LST–SST weakens and changes sign	All terms decay until nighttime values	Shear and thermal production terms similar, decreasing until they nullify at sunset	Pressure term weakens but stays positive (flow inland); turbulence not compensating

Table 2.1. Main features of the 5 phases during the simulated sea-breeze case (Cuxart et al., 2014).
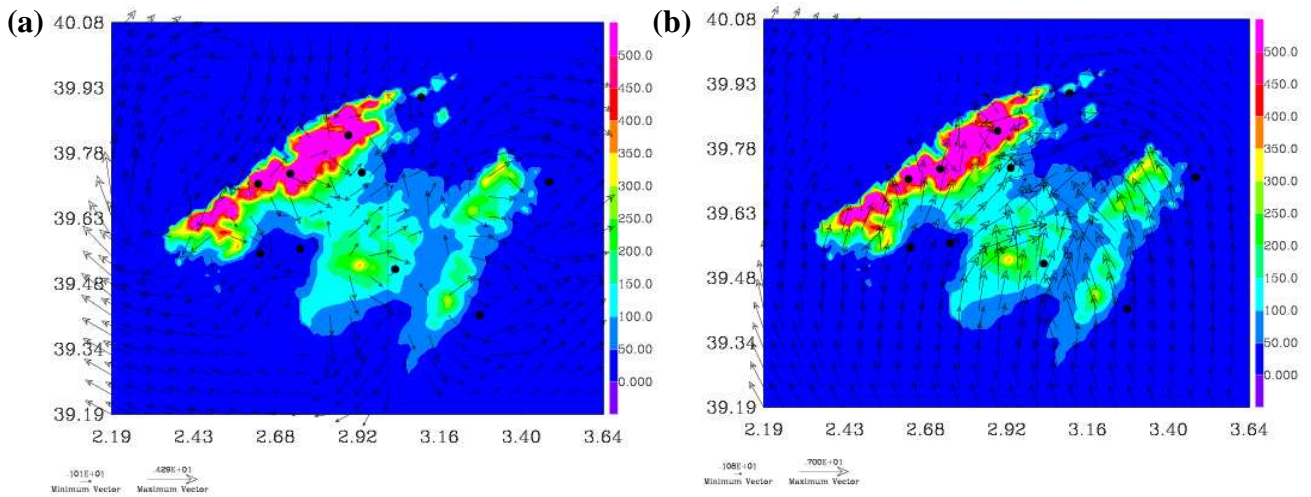
Figure 2.2. Wind vectors at 10m (a.g.l.) at (a) 0500 UTC on 5th June 2010 and at (b) 1200 UTC as an example of the land-breeze and sea-breeze periods, respectively.
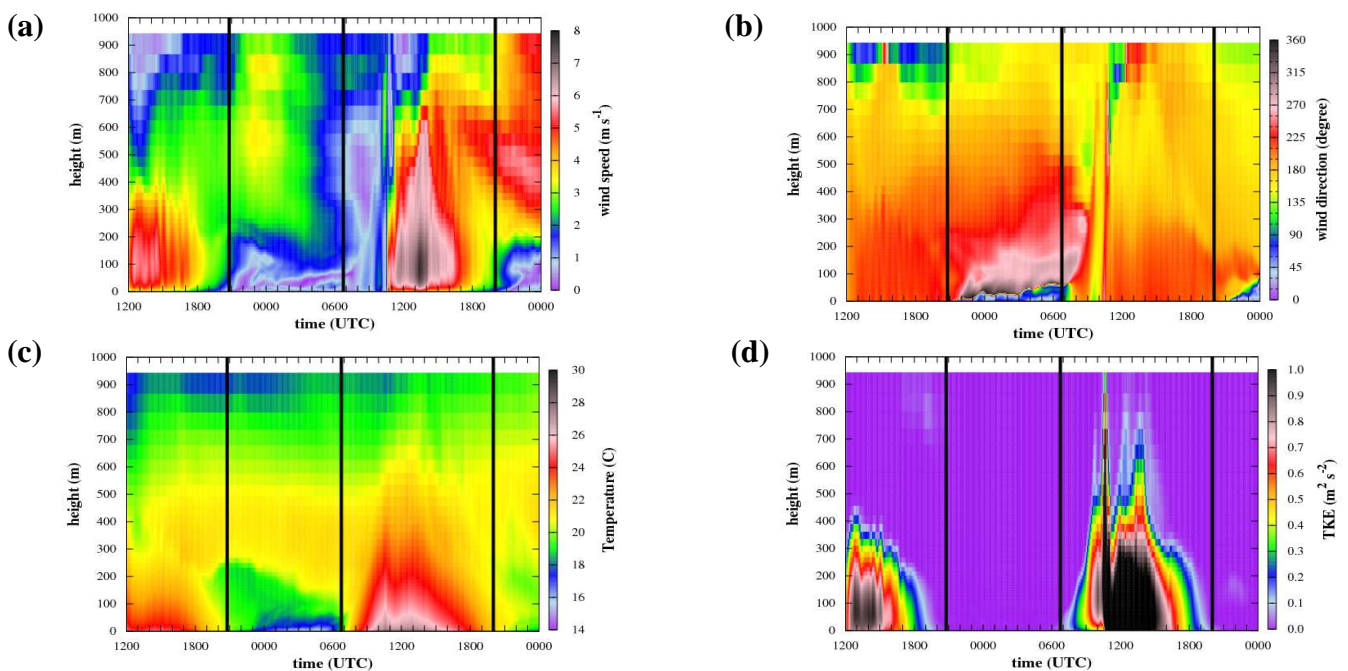

Figure 2.3. Time series of the vertical profiles obtained from the model in the location indicated with a red dot in Fig. 2.1 (where the experimental field campaigns will be performed).

The time evolution of some vertical profiles obtained from the model outputs are shown in Figure 2.3. When the sea-breeze is set, there is a layer of about 700m (a.g.l.) with wind direction from SW, the maximum intensity is around 100-200 m (a.g.l.) and the temperature profile corresponds to a well-mixed Convective Boundary Layer. TKE is large, mainly related to the strong updraft/downdrafts.

From the budget analysis it is found that the turbulence is the main warming mechanism whereas the cooling is mainly controlled by the advection (Fig. 2.4a and 2.4d). The vertical advection term is compensated by the horizontal one in the Budget of V (Fig. 2.4d). Thus, the total advection term in the budget is small in comparison to the turbulence or pressure. The largest contribution of the terms happens during the mature phase of the breeze (Fig. 2.4b and 2.4e). The budgets close to the coastline present sharp changes, being the terms larger over the land (Fig. 2.4c and 2.4f).
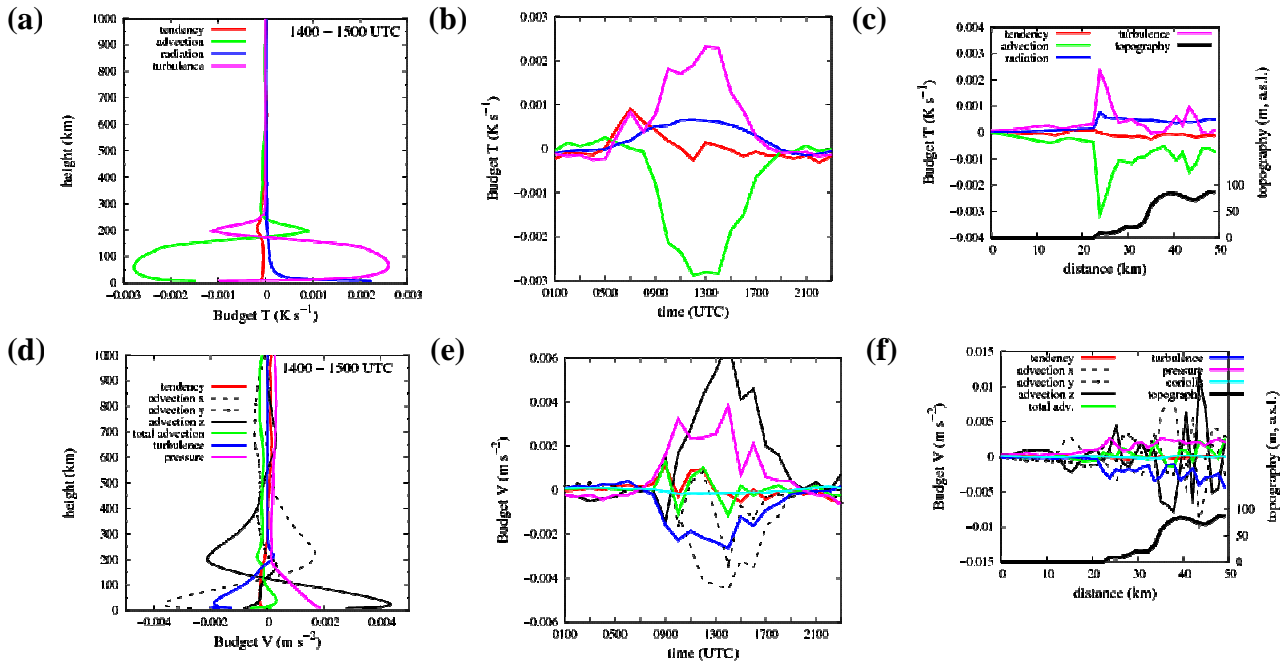
Figure 2.4. Temperature and wind speed budgets in the Campos basin (see location in the red point in Fig. 2.1). (a) and (d) Vertical profiles of the averaged budgets (from 1400 to 1500 UTC, mature phase). (b) and (e) Time series of the budgets at 10 m (a.g.l.). (c) and (f) Spatial evolution of the averaged terms (1400-1500 UTC) along the green line in Fig 2.1, together with the topography.

During the experimental field campaign MSB13 an IOP is selected to further explore the initiation of the Sea Breeze. A mesoscale simulation is performed, similar to the one presented above, and we are currently analysing the model outputs. The simulation is 24 h (starting on 19th September 2013) and it is verified with tethered balloon and multicopter observations (the measurement site is close to letter S Fig. 2.1) as it is seen in Figure 2.5.

The transition between LB and SB is seen to happen in four distinct steps: the land-breeze (transport of cold air from land over a warmer sea), the previous phase (the land progressively warms, but as long it is colder than the sea, the outland flow continues very similarly to the LB phase), the preparatory phase (the land becomes warmer than the sea surface and develops a convective boundary layer combined with upslope flows over the topography) and finally the development phase (the SB front propagates into the land through the central part of the basin). The main modelled and observed features are shown in Jiménez et al. (2015).
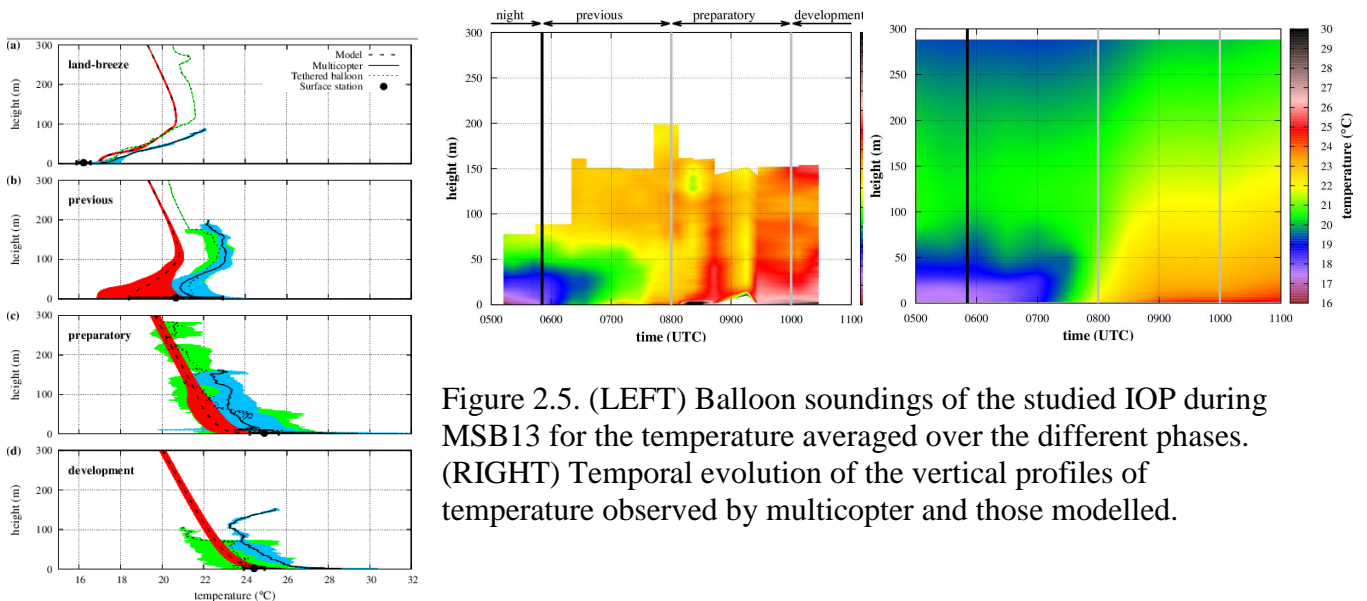

Figure 2.5. (LEFT) Balloon soundings of the studied IOP during MSB13 for the temperature averaged over the different phases. (RIGHT) Temporal evolution of the vertical profiles of temperature observed by multicopter and those modelled.

3) Strong nocturnal surface inversions

In clear nights with no well-defined synoptic pressure gradients, surface inversions may develop, with strong vertical temperature gradients in the first tens of meters above the surface. Usually these vertical gradients can be between 5 and 10 degrees in 10 or 20 meters and are misrepresented by numerical models and missed by most of fast ascending radiosoundings and ground-based remote sensing methods. Figure 3.1 shows the average of 16 soundings made just after sunset in Raimat, in the Eastern Ebro Valley, one clear night of February 2011 and the corresponding profiles from the simulation. There was a very large amount of condensation at the ground level that later freeze. The corresponding surface energy budget (Figure 3.2) shows a large imbalance in the first part of the night, when all these changes of phase take place. Our aim is to document well these cases observationally and to explore the simulations in order to find their weaknesses and propose ways of improvement.
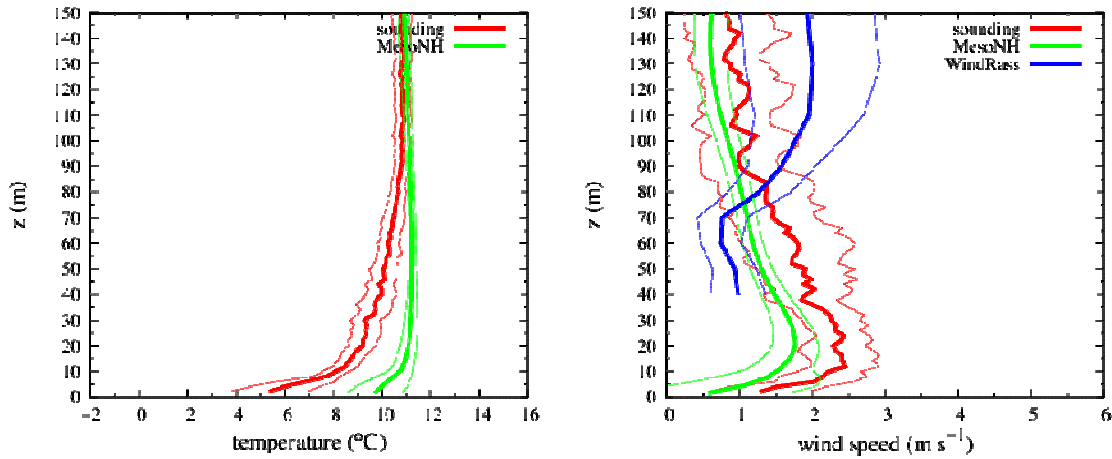

Figure 3.1. Observed and simulated soundings averaged over the evening.
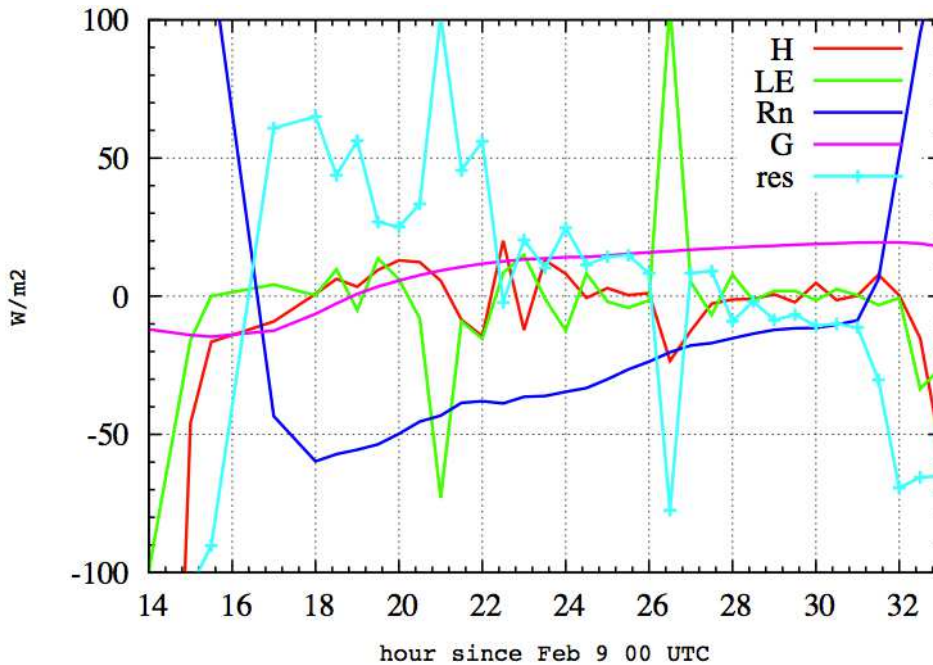

Figure 3.2. Observed surface energy balance in Raimat centered in the night 9-10 February.

Case in Mallorca (Feb 2012): During the night of 23 to 24 February 2012 there was a strong inversion event in the foothills in the Palma basin in the island of Mallorca. During that night, observations using a multicopter drone, a tethered balloon and surface data, were made at the campus of the University of the Balearic Islands (see location in Fig. 3.3). A high-resolution mesoscale simulation was performed, as the one described before, but with 3 nested domains of horizontal resolutions of 5km (covering the Balearic Islands, not shown), 1km (covering the island of Mallorca, see Fig. 2.1) and 250m (focusing in the measurement site at UIB indicated with a dot in Fig. 3.3).
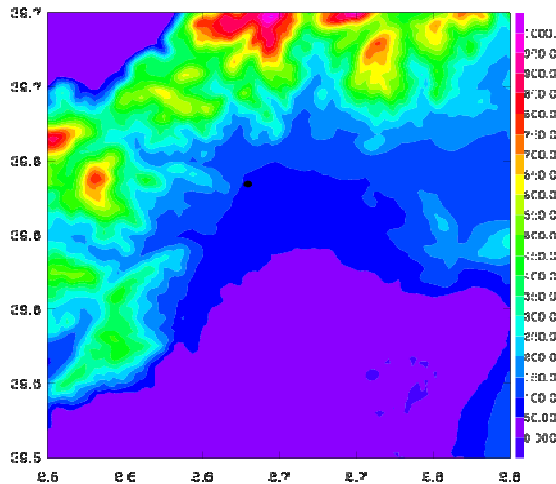

Figure 3.3. Topography of domain 3 (at 250m x 250m resolution) centered in the Campus of UIB (black dot) at the foothills of the northern mountain range and about 8km inland.

Preliminary results are show in Figures 3.4 and 3.5. It is found that during the night-time, at the campus of UIB the wind is from NE-E due to the downslope winds generated in the closest mountains. At around 0900 UTC the wind change the direction abruptly and during the day is from S due to upslope winds. The horizontal cross-sections show that at 250m resolution the topography is better captured that at 1km resolution.
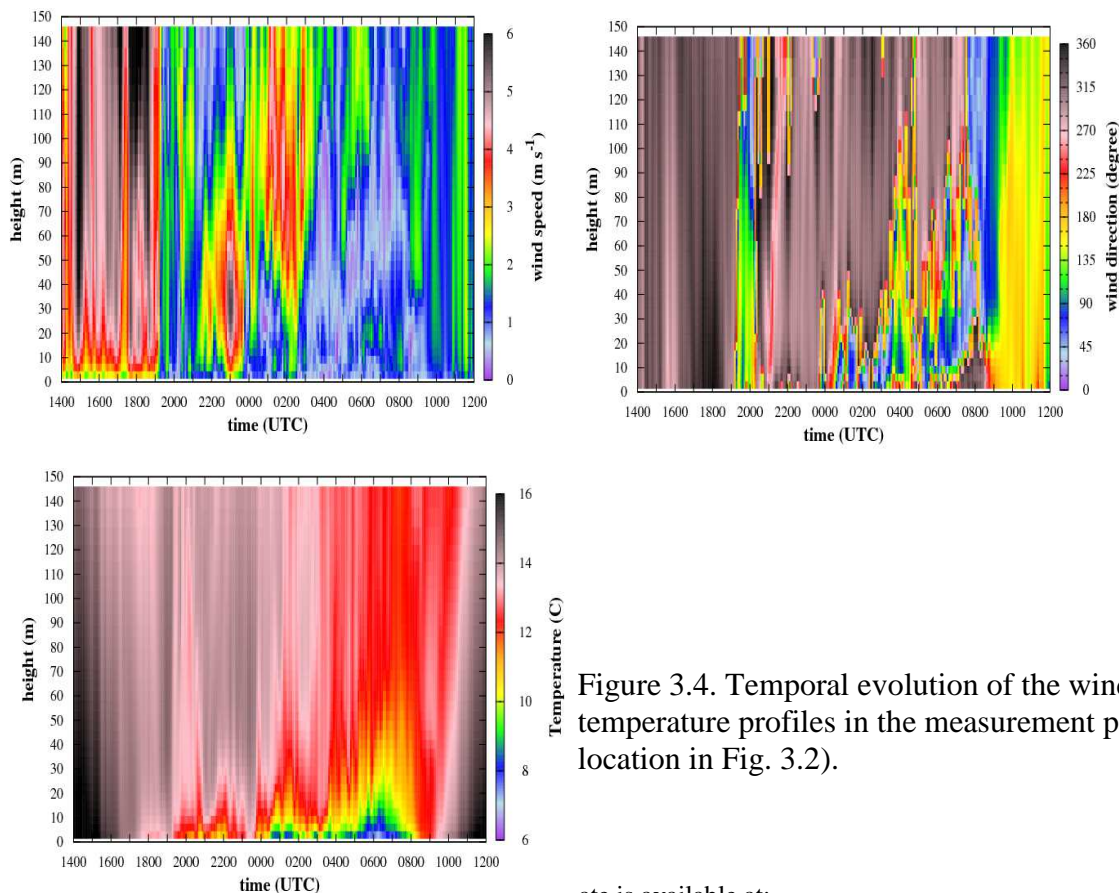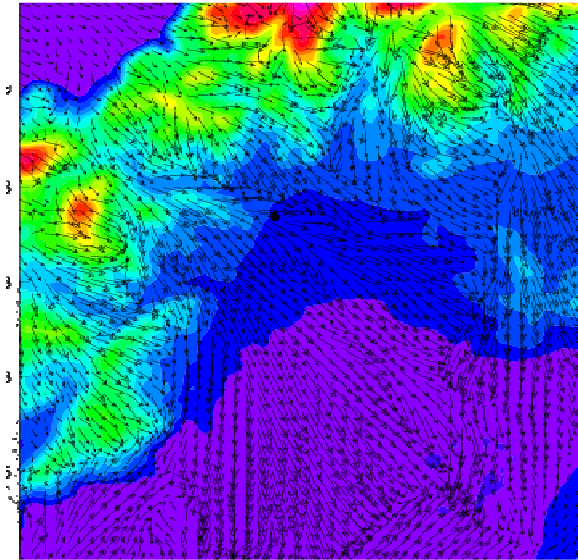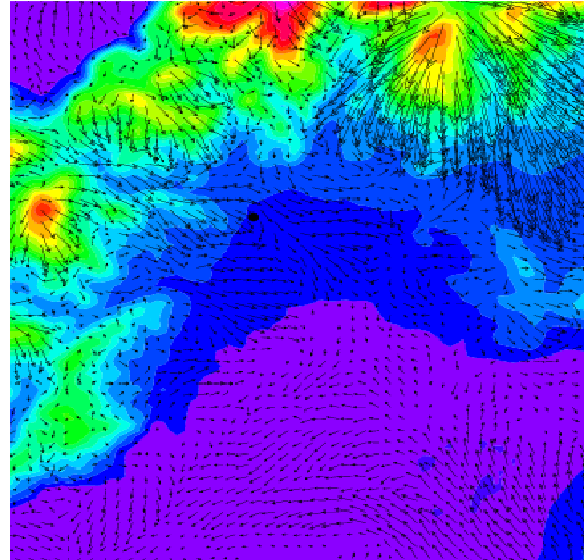

Figure 3.4. Temporal evolution of the wind and temperature profiles in the measurement point (see location in Fig. 3.2).
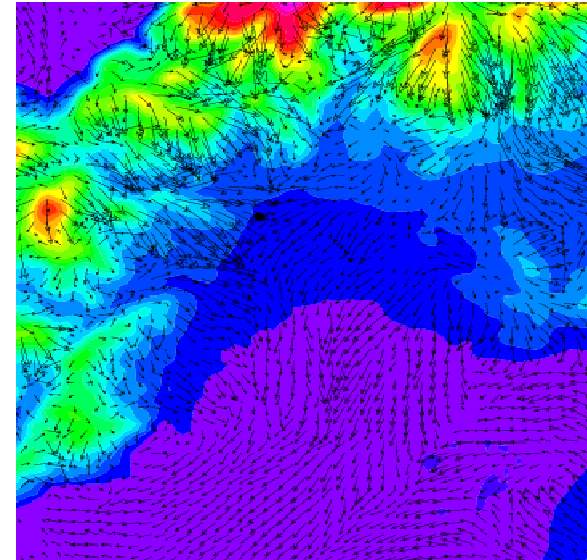
(a) 1600 UTC
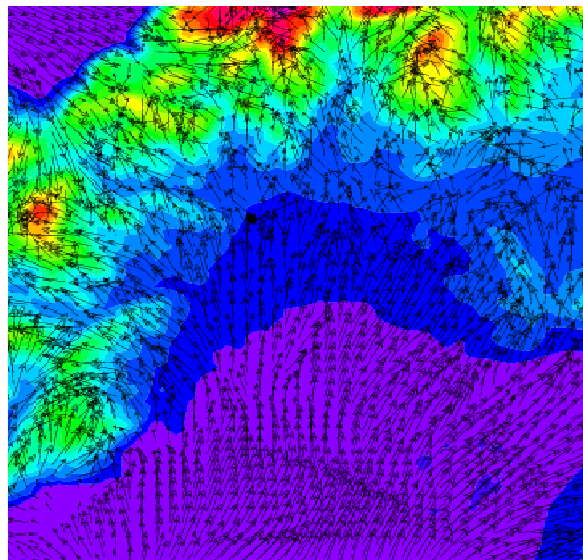
(b) 2200 UTC

(c) 0200 UTC

(d) 1200 UTC

Figure 3.5. Horizontal of the wind vectors at 10m (a.g.l.) at different instants.

Case in Raimat (Ebro Valley, Feb 2011): Several simulations over the Ebro river basin have been performed in the past to understand the dynamics of the basin under clear-skies nights and weak winds conditions. Typically this runs were made at 2km x 2km resolution and the chosen domain covered the whole basin.

A strong surface cooling event, like the one explained before, was observed during an experimental field campaign from 8th to 10th February 2011 in Raimat (placed in the northern dot in Figure 3.6). The setup of this run is like the previous cases studied in this basin except that now 2 nested domains are taken (see Figure 3.6), more centered in the area of interest.

Upslope/downslope winds are found in the elevated area where Raimat is located, in agreement with observations (Figures 3.7 and 3.8).

(a) Outer domain (1.2km x 1.2 km resolution)   **(b) Inner domain (300m x 300m resolution)**
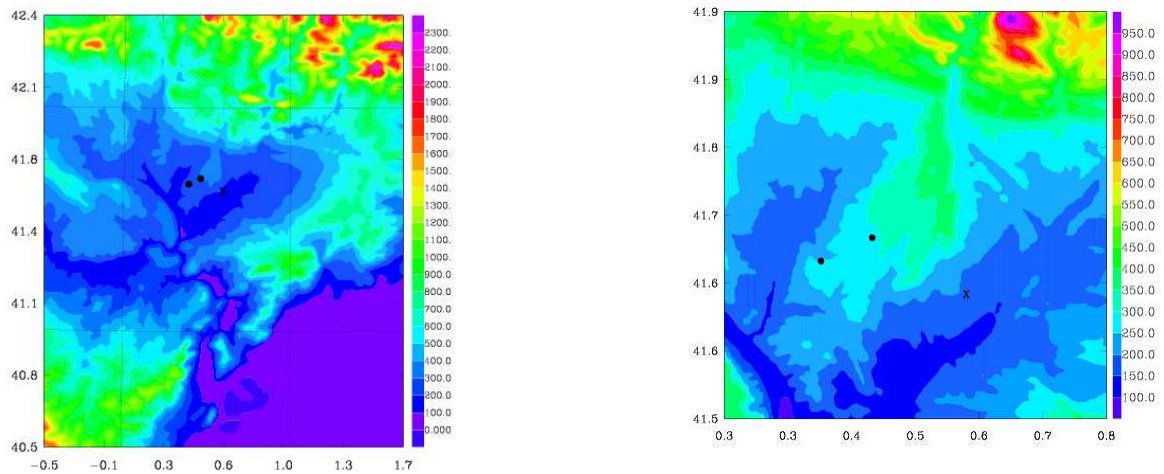
Figure 3.6. Inner and outer domains.

(a) 9 February 2011 at 0000 UTC   **(b) 9 February 2011 at 1200 UTC**
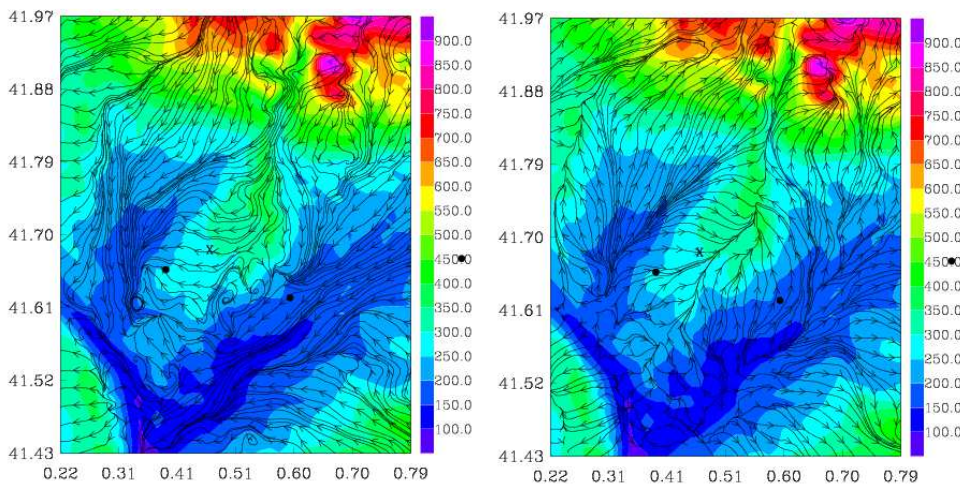

Figure 3.7. Streamlines at 15m (a.g.l.) obtained from the outer domain but for a zoom in the area of interest. The location of Raimat, where the experimental field campaign was done, is indicated with a cross.
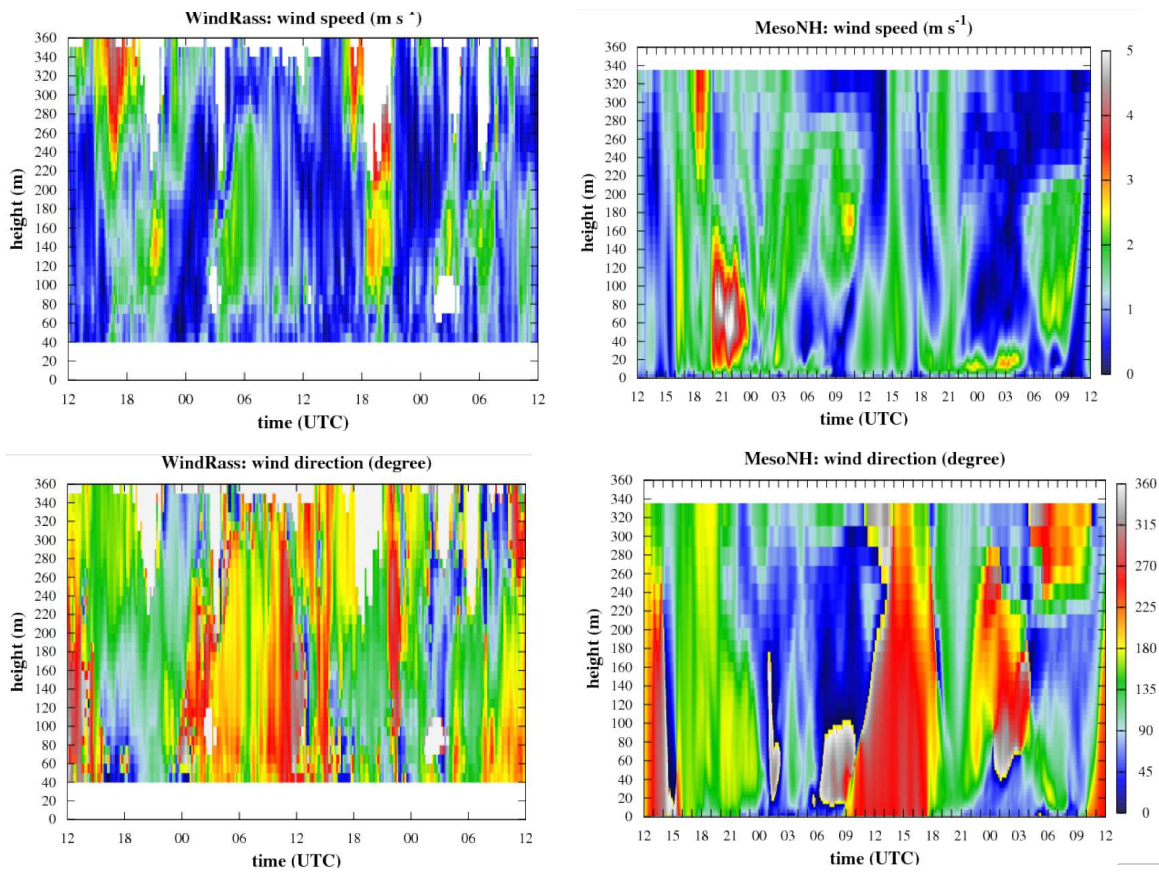
Figure 3.8. Time series of the vertical profiles of the wind speed and direction for Raimat during night 9-10 February 2011.

4) Analysis of the 24-h cycle in an Alpine valley

During August 2011, an experimental field campaign took place in the Reuss valley (Switzerland) with the main purpose to quantify the CH4 emissions at a farm scale (0.5-5 km2) in the ETH station of Chamau (see star in Figure 4.1). Apart from surface observations, manned and unmanned aircraft of Wintherthur's University (ZWAH) flew along and across valley, together with soundings in the experimental station of Chamau, belonging to the Swiss ETHZ.

A high-resolution mesoscale simulation is performed using 2 nested domains at 2km x 2km and 500m x 500m horizontal resolution and with a setup similar to the previous runs. The main objective of this run is to inspect what is the role of the slope and valley flows in the local energy budget at Chamau. The simulation start on August, 22nd 2011 at 0600 UTC and ends on August 24th, 2011 at 0000 UTC. Clear skies were reported during this period, allowing the development of topographically generated circulations. The computational cost is similar to the simulation in the Pyrenees explained in section 1 of this document.

(a) Outer domain (2km x 2km)   **(b) Inner domain (500m x 500m)**
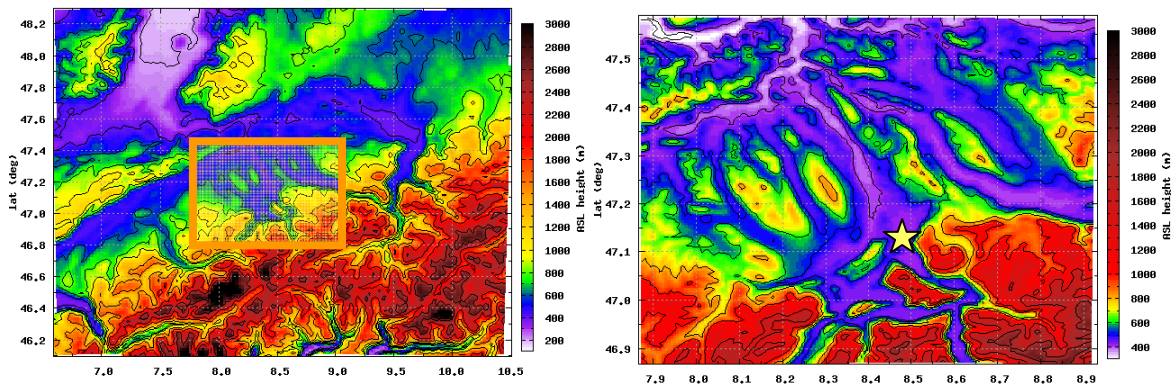
Figure 4.1. Topography of the inner and outer domains. The star indicated the location of Chamau, the main measurement site of the campaign.

(a)   **(b)**   **(c)**
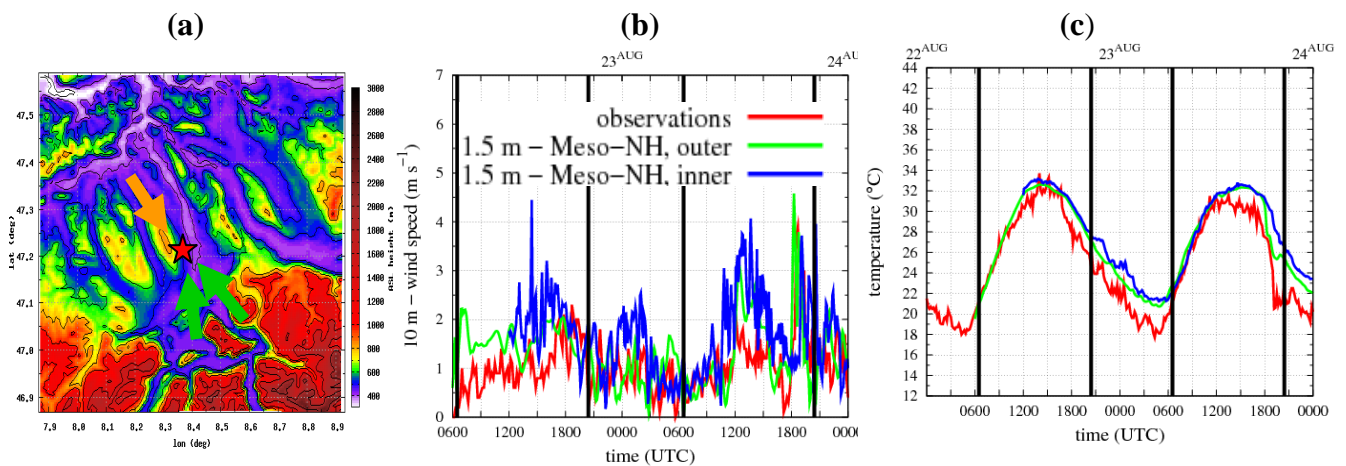
Figure 4.2. (a) Wind direction during the day (orange arrow) and during the night (green arrow) in Chamau (red start) obtained from the model outputs. (b) and (c) Comparison of the model results to the observations in Chamau.

From the horizontal cross-sections of the model outputs (not shown) it is seen that upslope and downslope winds are present during day and night, respectively, as it is sketched in the diagram in Fig. 4.2a. The model is able to reproduce this turning of the wind although it can be around 30min delayed, as it is seen in Fig. 4.3b. At higher levels, the model outputs agree with the observations from the manned and unmanned aircraft (Fig. 4.4). The wind speed is also well captured by the model at surface levels (Fig. 4.2b) and at higher levels (Figures 4.3 and 4.4).

(a) flight path from DIMO
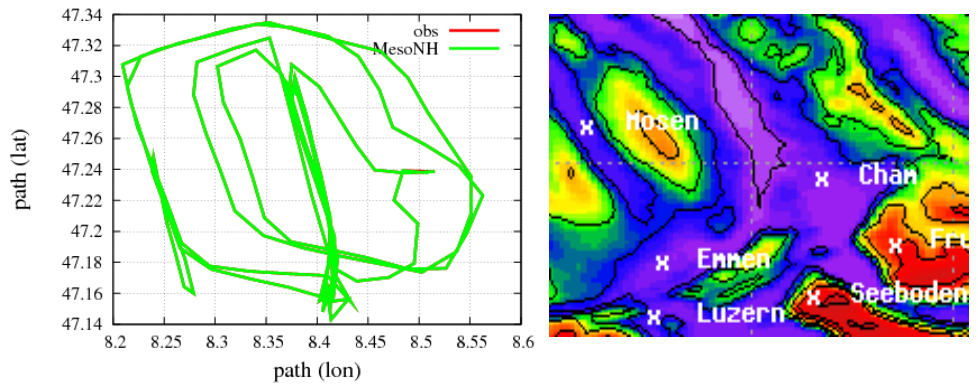
(b) Evening observations (1430 – 1730 UTC)
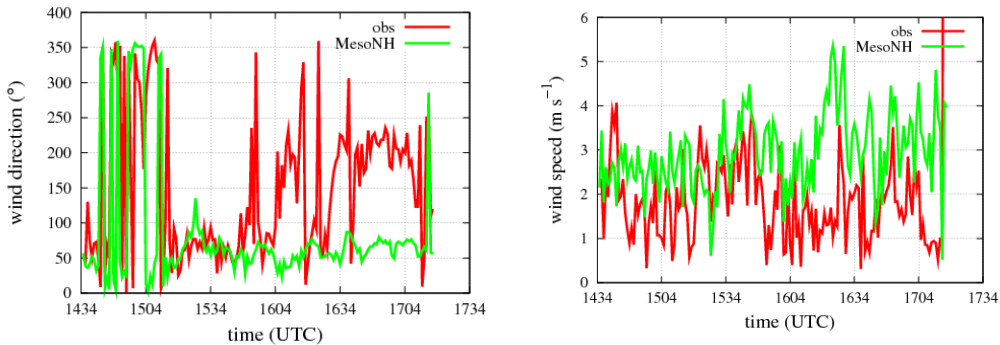
(c) Morning observations (0700 – 0930 UTC)
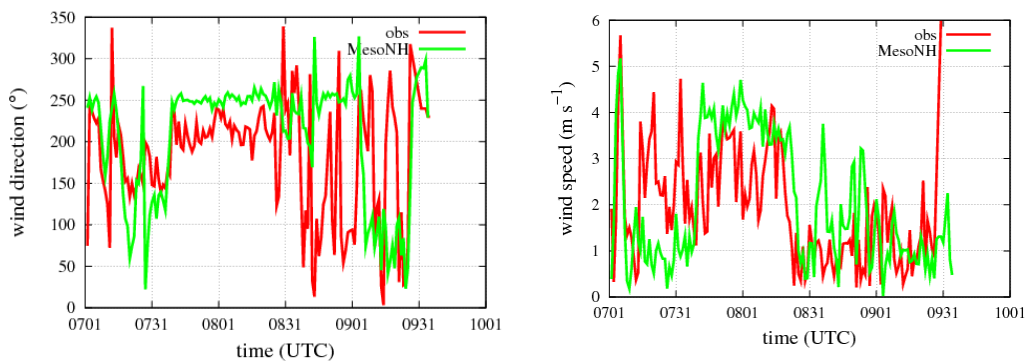
Figure 4.3. (a) Flight path of the measurement flights made by DIMO HB-2335, operated by MetAir AG during the experimental field campaign together with the topography of the area. (b) and (c) wind speed and direction observed (red line) during the evening and next morning, respectively, together with the model results (green line).
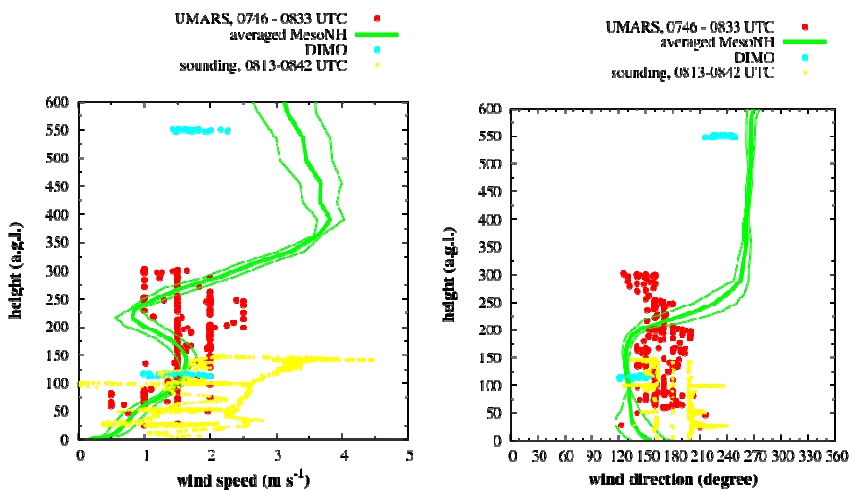
Figure 4.4. Comparison of the model (in green) and available observations: UAV in red, piloted aircraft in blue and profiles from the sounding in yellow. The model outputs are averaged over the period of the UMARS flight and in this plot is shown the mean value (thick green line) and the standard deviation (thin green line).

5) Surface Energy Budget Studies

DICE intercomparison case

During clear-sky and weak wind nights, most of the numerical weather prediction models have difficulties in reproducing the observations close to the surface, especially under strongly stratified conditions. One of the reasons is that the turbulence is weak and sometimes intermittent and thus difficult to parameterize in the models. In order to study the main physical processes that take place in the atmospheric boundary layer, and especially during the night, different model intercomparisons have been proposed, as the GEWEX Atmospheric Boundary Layer Study (GABLS) that we have participated. In GABLS, several regimes have been compared using 1D (Cuxart et al., 2006) and LES (Beare et al., 2006) models and in all the cases the initial profiles and the surface conditions (evolution of the temperature) are prescribed and based on observations.

The DIurnal land/atmosphere Coupling Experiment (DICE) is an international experiment designed to identify and understand the interactions and feedbacks between the land and atmospheric boundary layer. The GABLS2 experiment has been re-visited, but with the land surface community included within the analysis. This has allowed a multi-stage project whereby the sensitivity characteristics of each component (land and atmosphere) can be assessed and compared with the characteristics of the coupled simulations, as it is seen in Fig. 5.1. The DICE intercomparison case consists of 3 clear-sky days (72 hours) during the CASES99 campaign, with a variety of turbulence characteristics between them. The night-time regimes can be classified as intermittently turbulent, fully turbulent and very stable (hardly any turbulence) while the days also show differences in, for example, boundary layer growth rates. The participant models are shown in Fig. 5.1.

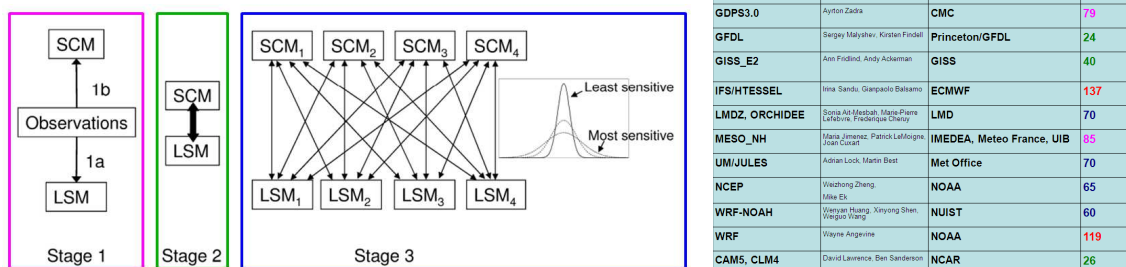| Model	Contact scientist	Institute	Levels
Arome & Arpege (NWP)	Eric Bazile	Meteo France	60/70
Arpege (CMIP5)	Isabelle Beau	Meteo France	
ECEARTH	Reinder Ronda, Bert Holtslag	Wageningen University	91
GDPS3.0	Ayrton Zadra	CMC	79
GFDL	Sergey Malyshev, Kirsten Findell	Princeton/GFDL	24
GISS_E2	Ann Fridlind, Andy Ackerman	GISS	40
IFS/HTESSEL	Irina Sandu, Gianpaolo Balsamo	ECMWF	137
LMDZ, ORCHIDEE	Sonia Ait-Mesbah, Marie-Pierre Lefebvre, Frederique Cheruy	LMD	70
MESO_NH	Maria Jimenez, Patrick LeMoigne, Joan Cuxart	IMEDEA, Meteo France, UIB	85
UM/JULES	Adrian Lock, Martin Best	Met Office	70
NCEP	Weizhong Zheng, Mike Ek	NOAA	65
WRF-NOAH	Wenyan Huang, Xinyong Shen, Weiguo Wang	NUIST	60
WRF	Wayne Angevine	NOAA	119
CAM5, CLM4	David Lawrence, Ben Sanderson	NCAR	26

Fig. 5.1. (LEFT) Simulation strategy of the DICE intercomparison case and (RIGHT) participant models.

Some of the results obtained from the MesoNH model are shown in Figure 5.2. It is found that for the coupled runs (Simple Column Model + Land Surface Model) the specific humidity is much larger than the observed, in good correspondence with larger latent heat flux (and smaller sensible heat flux) than the observed values. It is found that the root depth for this site (extracted from the climatologically database that the model has) it is too high. When the root depths are reduced to more realistic ones (more representative of the site) there is a better agreement between the model results and observations. We are currently preparing a manuscript (Jiménez et al., 2015b) to summarise some of the sensitivity tests made with the MesoNH model (such as the vertical grid, parameterizations used, …).
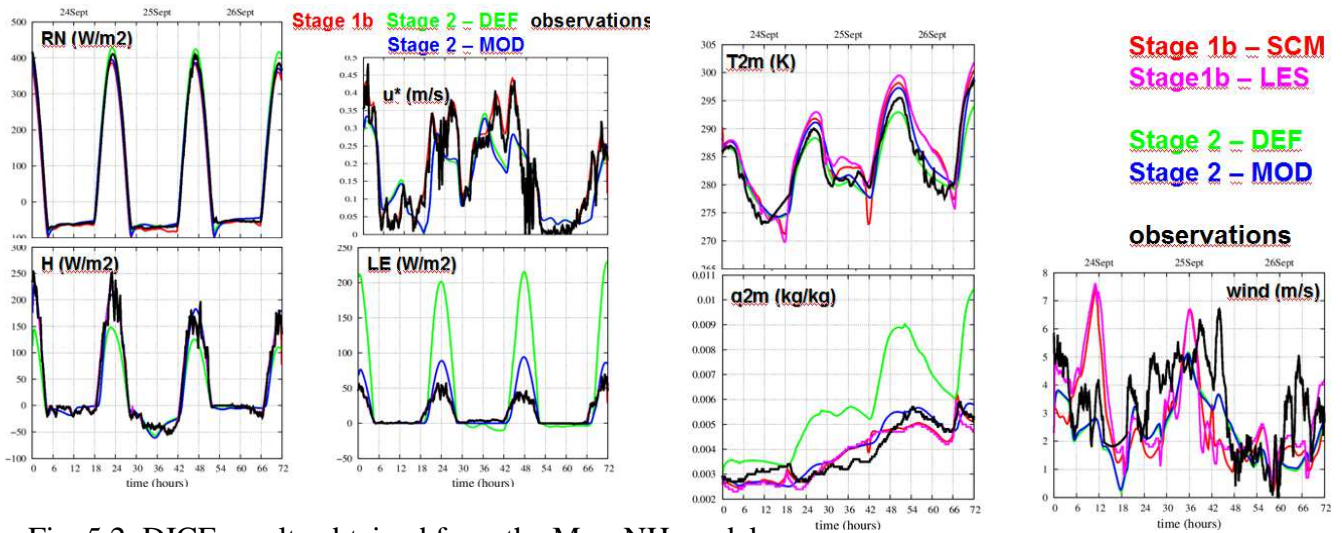
This template is available at:
http://www.ecmwf.int/about/computer_access_registration/forms/

Fig. 5.2. DICE results obtained from the MesoNH model.

Evaluation of the Surface Energy Budget Equation

Numerical atmospheric models force closure of the Surface Energy Budget (SEB), taking the ground flux as a residual. Taking the derivation of the SEB from the temperature equation (further explained in Cuxart et al., 2015) the imbalance can be written as:

$$Rnt + H - G - LE = - TT - A + S + B + Ot = Imb$$

where Rnt is the net radiation, H sensible heat flux, G the ground flux, LE the sensible heat flux, TT the temperature tendency, A the temperature advection , S the storage of the mass elements, B the biological processes and Ot other processes, such as instrumental errors. These terms have been estimated in Raimat (see location in Fig. 3.6) using data from a SEB station (2009-2010) and using the ECMWF model outputs at two instants: night (0000-0300 UTC) and day (1200-1500 UTC). Some of the results are shown in Table 5.1 and in Fig. 5.3.

It is found that irrigation is a common practice in this area and this input of water is not taken into account in the ECMWF model and this explains the differences between the modelled and observed surface energy balances (specially for the LE and H terms). On the other hand, the imbalance computed from the observations indicates that this contribution is important, especially during the night-time when this term is of the same order of magnitude as the other terms in the balance.

			TT	A	Rn_t	H	LE	G	Imb
1200-1500 UTC	annual	station	0.47	0.06	365.8	- 64.7	-155.9	-36.6	104.0
		model	0.23	-0.03	347.8	-148.6	-140.4	-58.9	0
	winter	station	0.37	0.07	180.1	- 50.8	-50.4	-23.2	59.4
		model	0.23	-0.06	186.1	-66.7	-76.9	-42.5	0
	spring	station	0.46	0.03	435.4	- 84.8	-185.8	-47.1	116.3
		model	0.23	-0.02	412.1	-180.2	-162.0	-70.0	0
	summer	station	0.62	0.11	555.9	- 65.2	-284.5	-57.1	142.5
		model	0.27	-0.02	509.3	-229.0	-204.2	-76.1	0
	fall	station	0.44	0.04	293.3	- 56.4	-104.8	-22.7	105.2
		model	0.17	-0.02	279.5	-116.3	-116.8	-46.3	0
0000-0300 UTC	annual	station	-0.29	0.21	-40.2	14.3	-7.5	23.0	-11.7
		model	-0.28	0.00	-56.7	13.7	-2.9	45.9	0
	winter	station	-0.16	0.25	-33.5	11.0	-4.3	19.2	-8.0
		model	-0.16	-0.05	-52.1	17.8	-1.8	36.1	0
	spring	station	-0.33	0.23	-41.8	15.3	-9.2	22.0	-14.6
		model	-0.33	0.01	-57.9	13.3	-3.6	42.8	0
	summer	station	-0.38	0.16	-47.6	21.2	-14.0	27.3	-15.4
		model	-0.37	0.04	-59.5	10.6	-3.5	52.4	0
	fall	station	-0.30	0.22	-38.1	9.9	-2.5	23.3	-8.9
		model	-0.24	-0.02	-57.3	13.2	-2.7	46.9	0

Table 5.1. Averaged observed and modelled values of the terms of the SEB (in W/m2); taking positive the flux to the surface.
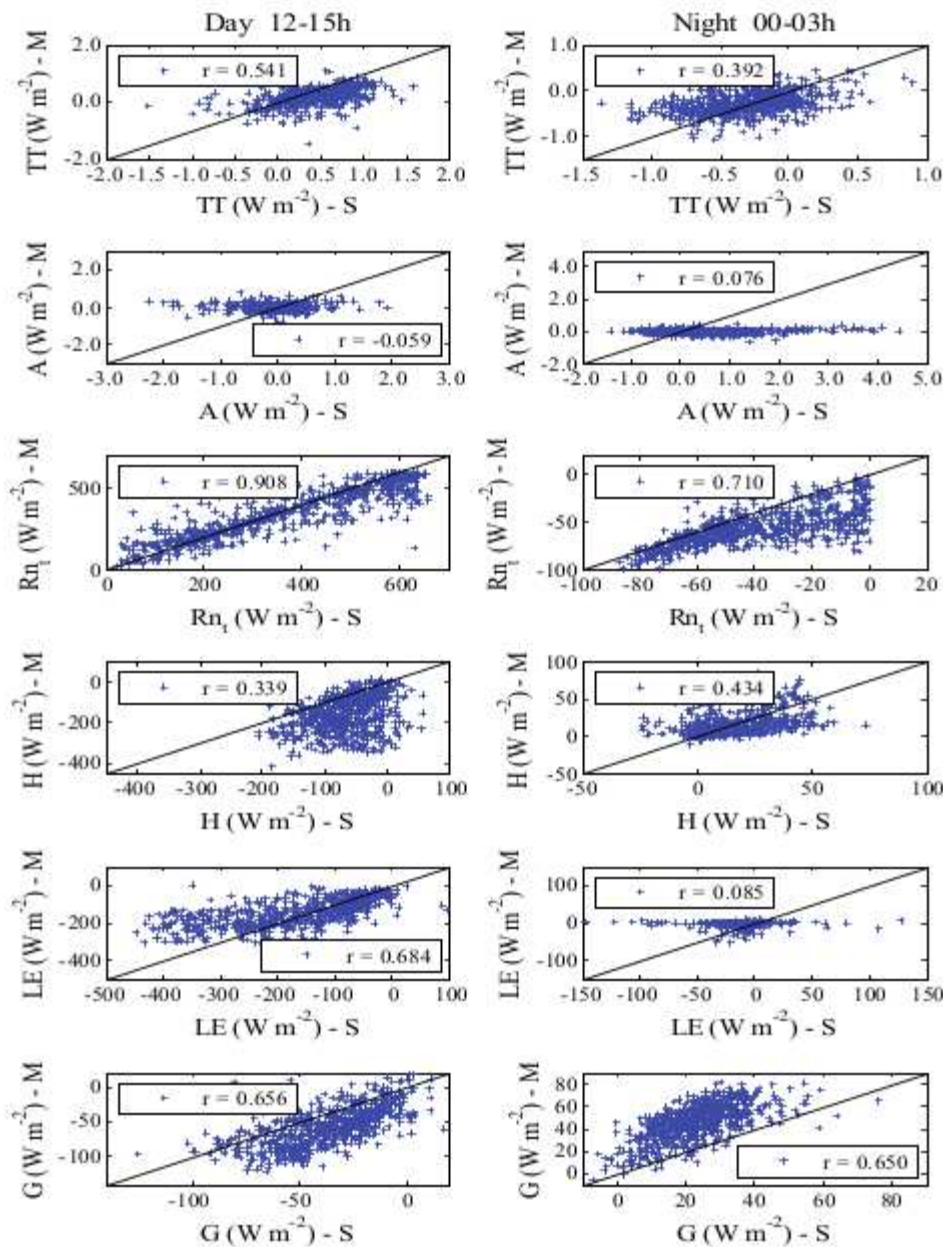
Fig. 5.3. Correlation between the observed values (labelled with S) with those simulated (M) for all the data during 2009 and 2010.

List of publications/reports from the project with complete references

Beare, R.J., MacVean, M.K., Holtslag, A.A.M., Cuxart, J., Esau, I., Golaz, J.-C., Jimenez, M.A., Khairoutdinov, M., Kosovic, B., Lewellen, D., Lund, T.S., Lundquist, J.K., McCabe, A., Moene, A.F., Noh, Y., Raash, S., and Sullivan, P., 2006: An intercomparison of Large-eddy simulations of the stable boundary layer. *Bound.-Layer Meteor.*, **118**, vol. 2, 247-272.

Bravo, M., Mira, A., Soler, M.R., and Cuxart, J., 2008: Intercomparison and evaluation of MM5 and Meso-NH mesoscale models in the stable boundary layer, *Bound.-Layer Meteor.*, **128**, 77-101.

Cuxart, J.; B. Wrenger; J. Dünnermann; D. Martínez; J. Reuder; M.O. Jonassen; M.A. Jiménez; M. Lothon; F. Lohou; O. Hartogensis; A. Garai; L. Conangla, 2015: Sub-kilometric heterogeneity effects on the surface energy budget in BLLAST. To be submitted to *Atmospheric Chemistry and Physics*.

Cuxart, J., Conangla, L. and Jiménez, M.A., 2015: Evaluation of the surface energy budget equation with experimental data and the ECMWF model in the Ebro valley. *J. Geophys. Res.*, **120**, 1008-1022.

Cuxart, J., Jiménez, M.A., Telisman-Prtenjak, M., and Grisogono, B., 2014: Study of a quasi-ideal sea breeze through momentum, temperature and turbulence budgets, *J. Appl. Meterol. and Clim.*, **53**, 2589-2609.

Cuxart, J., and Jiménez, M.A., 2012: Deep radiation fog in a wide closed valley: study by numerical modeling and remote sensing, *Pure and Applied Geophysics*, **169**, 911-926.

Cuxart, J., Cunillera, J., Jiménez, M.A., Martínez, D., Molinos, F., and Palau, J.L., 2012: Study of mesobeta basin flows by remote sensing, *Bound.-Layer Meteor.*, **143**, 143-158.

Cuxart, J., 2008: Nocturnal basin low-level jets: an integrated study, *Acta Geophysica,* **56**, 100-113.

Cuxart, J., and Jiménez, M.A., 2007: Mixing processes in a nocturnal Low-Level Jet: An LES study. *J. Atmos. Sci.*, **64**, vol. 5, 1666-1679.

Cuxart, J., Jiménez, M.A., and Martínez, D., 2007: Nocturnal katabatic and mesobeta basin flow on a midlatitude island. *Mon. Wea. Rev.*, **135**, vol. 3, 918-932.

Jiménez, M.A. and Cuxart, J., 2015: Slope winds during the BLLAST experiment. To be submitted to *Atmospheric Chemistry and Physics*.

Jiménez, M.A., LeMoigne, P., Couvreaux, F., and Cuxart, J., 2015b: The land-atmosphere coupling seen by the MesoNH model for the DICE case. To be submitted to *J. Hydrometeor.*

Jiménez, M.A., Simó, G., Wrenger, B., Telisman-Prtenjak; M., Guijarro, J.A., and Cuxart, J., 2015: Morning transition case between the land and the sea breeze regimes. Submitted to *Atmos. Res.*

Jiménez, M.A., and Cuxart, J., 2014: A study of the nocturnal flows generated in the north side of the Pyrenees, *Atmos. Res.*, **144-145**, 244-254.

Jiménez, M.A., Mira, A., Cuxart, J., Luque, A., Alonso, S., and Guijarro, J.A., 2008: Verification of a clear-sky mesoscale simulation using satellite-derived surface temperatures. *Mon. Wea. Rev.*, **136**, 5148-5161.

Jiménez, M.A., and Cuxart, J., 2005: Large-eddy simulations of the stable boundary layer using the standard Kolmogorov theory: range of applicability. *Bound.-Layer Meteor.*, **115**, 241-261.

M. Lothon, F. Lohou, D. Pino, F. Couvreux, E. R. Pardyjak, J. Reuder, J. Vilà-Guerau de Arellano, P. Durand, O. Hartogensis, D. Legain, P. Augustin, B. Gioli, I. Faloona, C. Yagüe, D. C. Alexander, W. M. Angevine, E. Bargain, J. Barrié, E. Bazile, Y. Bezombes, E. Blay-Carreras, A. van de Boer, J. L. Boichard, A. Bourdon, A. Butet, B. Campistron, O. de Coster, **J. Cuxart**, A. Dabas, C. Darbieu, K. Deboudt, H. Delbarre, S. Derrien, P. Flament, M. Fourmentin, A. Garai, F. Gibert, A. Graf, J. Groebner, F. Guichard, **M. A. Jimenez**, M. Jonassen, A. van den Kroonenberg, D. H. Lenschow, V. Magliulo, S. Martin, D. Martinez, L. Mastrorillo, A. F. Moene, F. Molinos, E. Moulin, H. P. Pietersen, B. Piguet, E. Pique, C. Román-Cascón, C. Rufin-Soler, F. Saïd, M. Sastre-Marugán, Y. Seity, G. J. Steeneveld, P. Toscano, O. Traullé, D. Tzanos, S. Wacker, N. Wildmann, and A. Zaldei, 2014: The BLLAST field experiment: Boundary-Layer Late Afternoon and Sunset Turbulence. *Under revision in Atmos. Chem. Phys. Discuss*.

Martínez, D., Jiménez, M.A., Cuxart, J., and Mahrt, L., 2010: Heterogeneous nocturnal cooling in a large basin under very stable conditions. *Bound.-Layer Meteor., 137, 97-113.*

Martínez, D., and Cuxart, J., 2009: Assessment of the hydraulic slope flow approach using a mesoscale model, *Acta Geophysica*, **57**, 882-903.

Martínez, D., and Cuxart, J., and Cunillera, J., 2008: Climatologia condicionada de les nits establement estratificades al pla de Lleida, *Tethys*, **5**, 13-24.

Martínez, D., and Cuxart, J., 2007: A gravity current study within the Palma de Mallorca basin. *Física de la Tierra*, **19**, 21-36.

Future plans
(Please let us know of any imminent plans regarding a continuation of this research activity, in particular if they are linked to another/new Special Project.)

The continuation of this special project is linked to the current special project EFFECT OF THE SURFACE HETEROGENEITIES IN THE ATMOSPHERIC BOUNDARY-LAYER (2015-2017) where the simulations will continue support the experimental field campaigns that we organize/collaborate to further understand the physical processes that take place under sea/land breezes and the slope winds regimes.